Comparison of liquid-phase olefin epoxidation catalysed by dichlorobis-(dimethylformamide)dioxomolybdenum(VI) in homogeneous phase and grafted onto MCM-41

Bernardo Monteiro[a], Salete S. Balula[a], Sandra Gago[a], Carla Grosso[b], Sónia Figueiredo[b], André D. Lopes[b,*], Anabela A. Valente[a], Martyn Pillinger[a], João P. Lourenço[b], Isabel S. Gonçalves[a,**]

[a] Department of Chemistry, CICECO, University of Aveiro, 3810-193 Aveiro, Portugal
[b] Faculty of Science and Technology, CIQA, University of the Algarve, Campus de Gambelas, 8005-139 Faro, Portugal

ARTICLE INFO

ABSTRACT

A mesoporous silica-supported molybdenum oxide catalyst with a loading of 0.17 Mo/nm^2 was prepared by liquid phase deposition of MoO$_2$Cl$_2$(dmf)$_2$ (**1**) onto MCM-41 (dmf = dimethylformamide). Powder X-ray diffraction and N$_2$ adsorption studies of Mo-MCM-41 indicate that the texture properties of the support were preserved during the grafting experiment. On the basis of evidence from FTIR spectroscopy, ^{13}C and ^{29}Si MAS NMR, and Mo K-edge EXAFS, the Mo atoms in this catalyst are mainly present as isolated {MoO$_2$[(–O)$_3$SiO]$_2$(dmf)$_2$} species, with a small contribution from oxo-bridged dimers. Catalysis tests show that complex **1** and Mo-MCM-41 are highly active oxidation catalysts for liquid-phase epoxidation of unfunctionalised olefins using *tert*-butylhydroperoxide as oxidant, from ambient to 55 °C. The high stability and recyclability of the heterogeneous Mo-MCM-41 catalyst is attributed to the strong metal oxide–support interaction. With cyclooctene, 1-octene, *trans*-2-octene and norbornene substrates, the corresponding epoxides were the only observed reaction products. The reactions of the other substrates gave by-products such as 8,9-*p*-menthen-1,2-diol from (*R*)-(+)-limonene, campholenic aldehyde from α-pinene, and benzaldehyde from styrene. The addition of dichloromethane as a co-solvent had a beneficial effect on catalytic performance, and in the case of (*R*)-(+)-limonene allowed the epoxide to be formed as the only reaction product.

1. Introduction

Silica-supported molybdena (MoO$_x$) catalysts have attracted considerable attention in recent years due to their activity for a variety of industrially important reactions, such as the selective oxidations of alkanes [1], alkenes [2] and alcohols [3]. The catalytic performance depends to a large extent on the molecular structure of the supported species, which in turn depends on the preparation method, the nature of the silica support, the Mo surface concentration, the pre-treatment conditions, and the state of hydration [4]. At low coverage, the active sites have been proposed to have various structures, including isolated mono-oxo, dioxo and dimeric surface species [3c,5,6], while at high coverage, Mo may be present as polymolybdate domains and MoO$_3$ crystallites [7].

The coexistence of multiple Mo structures makes it difficult to determine structure–reactivity correlations. Hence, considerable effort has been directed towards the study of isolated molybdate species dispersed on silica [5d]. From a catalytic point of view, these systems are of special interest due to the possibility of obtaining single-site heterogeneous catalysts [8]. One way to achieve high dispersions is to use low nuclearity Mo precursors, for example MoCl$_5$ [9], Mo(η^3-C$_3$H$_5$)$_4$ [2b,9a], (η^5-C$_5$H$_5$)$_2$Mo$_2$(CO)$_6$ [2b], Mo$_2$(η^3-C$_3$H$_5$)$_4$ [6a,9a,10], Mo$_2$(OAc)$_4$ [11], MoO$_2$(acac)$_2$ [12], (η^5-C$_5$H$_5$)$_2$MoCl$_2$ [13], MoO[OSi(O^{t}Bu)$_3$]$_4$ [5b] and MoO(O$_2$)$_2$(H$_2$O)$_2$ [2c,7c], which lead to surface-fixed species such as (≡Si–O)$_2$Mo(η^5-C$_5$H$_5$)$_2$, (≡Si–O)MoO[OSi(O^{t}Bu)$_3$]$_3$ and (≡Si–O)MoOH(O$_2$)$_2$. These decompose during thermal treatments to give discrete tetrahedral oxomolybdenum species like (≡Si–O)$_2$MoO$_2$. When the complex MoO$_2$Cl$_2$(thf)$_2$ (thf = tetrahydrofuran) was used to derivatise MCM-41, an ordered mesoporous silica, a final calcination step was not necessary because the substitution of the chloro ligands by siloxy groups from the silica surface gave rise to surface-fixed dioxomolybdenum(VI) species in one step (albeit with auxiliary coordinated thf molecules) [3c]. The grafted material exhibited fair

---

* Corresponding author.
** Corresponding author. Tel.: +351 234 378190; fax: +351 234 370084.
E-mail addresses: adlopes@ualg.pt (A.D. Lopes),
igoncalves@ua.pt (I.S. Gonçalves).

activity and selectivity for liquid-phase olefin epoxidation using *tert*-butylhydroperoxide (*t*BuOOH) as the oxidant, although one run was necessary to obtain steady catalytic activity and a stable catalyst. When triethylamine was used in the grafting reactions to activate the surface silanol groups, a material with a higher Mo loading was obtained, and Mo K-edge EXAFS studies indicated the presence of surface dioxo(μ-oxo)molybdenum(VI) dimeric species. While this material was not very active as a catalyst for olefin epoxidation, good results were obtained for the oxidation of secondary aliphatic and benzylic alcohols.

The complex $MoO_2Cl_2(thf)_2$ belongs to a large family of solvent adducts with the general formula $MoO_2X_2(S)_2$ (X = F, Cl, Br; S = thf, dmf, dmso, CH_3CN, H_2O) [14]. Of these, the complex $MoO_2Cl_2(dmf)_2$ (**1**) (dmf = dimethylformamide) has been investigated as a catalyst for several organic transformations, such as the epoxidation of olefins [15], the oxidation of alcohols [16], and the reductive cyclisation of nitrobiphenyls and nitrostyrenes to carbazoles and indoles [17]. In the present paper, we report on (1) the catalytic performance of **1** for the epoxidation of several olefins using *t*BuOOH as oxidant, (2) the influence of temperature, substrate/oxidant molar ratio, nature of oxidant (*t*BuOOH, cumene hydroperoxide (CuOOH) or H_2O_2) and solvent on the catalytic performance of **1** for the epoxidation of cyclooctene, (3) the synthesis and characterisation of MCM-41 derivatised with **1**, and (4) the catalytic performance of the derivatised material for the epoxidation of several olefins using *t*BuOOH as oxidant. Particular attention is paid to the question of leaching of active species from the mesoporous catalyst and the homogeneous/heterogeneous nature of the catalytic process, as well as the reuse of the catalyst.

2. Experimental

2.1. Materials and methods

All air-sensitive operations were carried out using standard Schlenk techniques under nitrogen with solvents dried by standard procedures. Purely siliceous MCM-41 was synthesised as described previously using hexadecyltrimethylammonium chloride as the templating agent [18]. The template was partially removed by extraction with a solution of 0.1 M NH_4NO_3 (Merck) in 96% ethanol at reflux temperature for 2 h. After drying, the product was calcined under dry air at 550 °C for 10 h. The temperature was increased from 25 to 550 °C at 1 °C min^{-1}. Powder XRD ($h\,k\,l$ in parentheses): $2\theta(°)$ = 2.15 (1 0 0), 3.71 (1 1 0), 4.29 (2 0 0), 5.77 (2 1 0); $a = 2d_{100}/\sqrt{3}$ = 47.4 Å.

ICP-AES analysis for Mo was performed at the Central Laboratory for Analysis, University of Aveiro (by L. Carvalho), and microanalyses for CHN were carried out at the Department of Chemistry, University of Aveiro (by M.F. Lucas). Powder XRD data were collected on an X'Pert MPD Philips diffractometer (Cu Kα X-radiation, λ = 1.54060 Å) fitted with a curved graphite monochromator and a flat plate sample holder, in a Bragg-Brentano para-focusing optics configuration (40 kV, 50 mA). Samples were step-scanned in 0.02° 2θ steps with a counting time of 2 s per step. The BET specific surface area (p/p_0 from 0.03 to 0.13) and specific total pore volume were estimated from N_2 adsorption isotherms measured at -196 °C, using a gravimetric (sub-atmospheric) adsorption apparatus equipped with a CI electronic MK2-M5 microbalance and an Edwards Barocel pressure sensor. Before the measurements, MCM-41 and Mo-MCM-41 were outgassed at 300 and 120 °C, respectively, and maintained at that temperature overnight to a residual pressure of ca. 10^{-4} mbar. The pore size distributions (PSD) were computed from the adsorption branch of the experimental isotherms by the BJH method using the modified Kelvin equation

and a correction for the statistical film thickness on the pore walls [19].

FTIR spectra using KBr pellets were obtained on a Mattson-7000 infrared spectrophotometer with 2 cm^{-1} resolution. FT Raman spectra were recorded on a RFS-100/S Bruker FT-spectrometer, using a Nd:YAG laser (Coherent compass-1064/500) with an excitation wavelength of 1064 nm and 4 cm^{-1} resolution. ^{1}H NMR spectra were obtained using a Bruker CXP 300 spectrometer. Solid-state magic-angle-spinning (MAS) NMR spectra were recorded at 79.49 MHz for ^{29}Si and 125.76 MHz for ^{13}C on Bruker Avance 400/500 spectrometers. ^{29}Si MAS NMR spectra were recorded with 40° pulses, spinning rates of 5.0–7.0 kHz and 60 s recycle delays. ^{29}Si CP MAS NMR spectra were recorded with 5.5 μs ^{1}H 90° pulses, 8 ms contact time with a spinning rate of 5 kHz and 4 s recycle delays. ^{13}C CP MAS NMR spectra were recorded with 4.5 μs ^{1}H 90° pulses and 2 ms contact time with a spinning rate of 7.0 kHz and 4 s recycle delays. Chemical shifts are quoted in parts per million from tetramethylsilane.

Mo K-edge X-ray absorption spectra were measured at room temperature in transmission mode on Station 16.5 at the Daresbury Laboratory Synchrotron Radiation Source (DL SRS), operating at 2 GeV with currents between 170 and 200 mA. The order-sorting double Si(2 2 0) crystal monochromator was detuned to 70% of its maximum response to suppress harmonic contamination of the signal. Solid samples were diluted if necessary with BN and pressed into 13 mm pellets. Scans were set up to record the pre-edge at 10 eV steps and the post-edge region in 0.04 Å^{-1} steps, giving a total acquisition time of ca. 40 min per scan. Scans were summed to improve the data quality. The programs EXCALIB (DL SRS) and PYSPLINE [20] were used for calibration and background subtraction of the raw data. EXAFS curve-fitting analyses, by least-squares refinement of the non-Fourier filtered k^3-weighted EXAFS data, were carried out using the program EXCURVE (version EXCURV98 [21]) using fast curved wave theory [22]. The calculations were performed using single scattering contributions. Phase shifts were obtained within this program using ab initio calculations based on the Hedin Lundqvist/von Barth scheme. For each EXAFS simulation the validity of extra parameters was checked using a comparative reduced χ^2 method [23].

2.2. $MoO_2Cl_2(dmf)_2$ (**1**) [14c]

A stirred mixture of MoO_3 (10 g, 69.5 mmol) and 6 M HCl (100 mL) was heated near the boiling point until most of the MoO_3 was dissolved, then cooled to room temperature and filtered. Freshly distilled dmf (25 mL) was added to the filtrate with stirring and the resultant microcrystalline precipitate was collected by filtration, washed with acetone (50 mL) and dried under vacuum. Yield: 21.2 g, 88%. Anal. calcd for $C_6H_{14}N_2Cl_2MoO_4$ (345.03): C, 20.89; H, 4.09; N, 8.12. Found: C, 20.49; H, 3.89; N, 7.95. FTIR (KBr, cm^{-1}): 2947 m, 1653vs, 1488 m, 1434vs, 1374vs, 1246s, 1118s, 1055m, 1008 m, 942vs, 902vs, 683vs, 416 m, 397 s, 389 s, 378 s, 338 s. Raman (cm^{-1}): 3016, 2986, 2942, 2827, 1646, 1493, 1436, 1425, 1376, 1120, 938, 905, 865, 689, 683, 419, 390, 378, 311, 260, 225, 150, 127, 85. ^{1}H NMR (300 MHz, 298 K, CD_2Cl_2, TMS): δ = 7.89 (s, 1H), 2.84 (s, 3H), 2.75 (s, 3H). ^{13}C CP MAS NMR: δ = 167.3 (C=O), 38.4 (N–CH_3), 32.1 (N–CH_3).

2.3. Mo-MCM-41

After removing physisorbed water from calcined MCM-41 (2 g) by heating at 120 °C under reduced pressure for 2 h, a solution of **1** (1.05 g, 3.0 mmol) in CH_2Cl_2 (80 mL) was added and the mixture stirred at room temperature overnight. The solution was filtered off and the resultant pale blue powder washed with CH_2Cl_2

(3×30 mL), and dried under reduced pressure at room temperature for several hours. Anal. found: Mo, 2.21; C, 3.49; H, 1.18; N, 0.82. FTIR (KBr, cm^{-1}): 3453br, 2942w, 1654m, 1438w, 1384w, 1235m, 1081vs, 970br, 910sh, 801m, 565br, 458m. ^{13}C CP MAS NMR: δ = 164.2 (C=O), 35.6 (N–CH$_3$), 30.1 (N–CH$_3$). ^{29}Si MAS NMR: δ = −109.1 (Q^4) [Q^n = Si(OSi)$_n$(OH)$_{4-n}$]. ^{29}Si CP MAS NMR: δ = −101.5 (Q^3), −109.3 (Q^4).

2.4. Catalytic oxidation reactions

The liquid-phase catalytic oxidations were carried out in a closed Pyrex reaction vessel equipped with a magnetic stirrer and immersed in a thermostated oil bath. A 1% molar ratio of complex/substrate and a substrate/oxidant molar ratio of either 1:1 or 1:1.6 were used. The oxygen donors were *t*BuOOH (5.5 M in decane), CuOOH (80% in cumene) or 30% aqueous H$_2$O$_2$. The reactions were carried out at either 25 or 55 °C, without additional solvent or with *n*-hexane, CH$_2$Cl$_2$ or dmf (1.2 L co-solvent per mol of olefin). The reaction courses were monitored using a Varian 3900 GC equipped with a capillary column (DB-5, 30 m × 0.25 mm, or CP WAX 52CB, 30 m × 0.53 mm) and a flame ionisation detector. The products were identified by GC–MS (HP 5890 Series II GC and HP 5970 Series Mass Selective Detector) using He as carrier gas.

3. Results and discussion

3.1. Synthesis and characterisation

Dichlorobis-(dimethylformamide)dioxomolybdenum(VI) (**1**) was prepared as described previously by treatment of an aqueous hydrochloric acid solution of MoO$_3$ with excess dmf [14c], and gave satisfactory elemental analysis and infrared and NMR spectra. Exposure of calcined and dehydrated MCM-41 to a dichloromethane solution of **1** gave the derivatised material Mo-MCM-41 as a pale blue powder, with a surface coverage of 0.17 Mo/nm^2 based on the metal loading of 2.21 wt.% and a surface area of 811 m^2 g^{-1} (see below). Elemental analysis of Mo-MCM-41 gave an N/Mo molar ratio of 2.5, which suggests that the dmf molecules initially present in **1** were retained in the grafted material.

Fig. 1 shows the powder XRD patterns of the MCM-41 starting material and the modified material Mo-MCM-41. The pattern for MCM-41 is characteristic of a well-ordered mesoporous phase and can be indexed as hexagonal with a lattice parameter of 47.4 Å (=2d_{100}/$\sqrt{3}$). The Bragg peaks indexed as (1 0 0), (1 1 0), (2 0 0) and (2 1 0) are still observed at the same 2θ values after the derivatisation step, which indicates retention of the long-range hexagonal symmetry. Compared with MCM-41, the intensity of the (1 0 0) reflection is noticeably less intense. Although a loss of structural order could be the cause of this change, it is more likely that the introduction of the Mo complex inside the channels of the support affects the peak intensity by reducing the X-ray scattering contrast between the silica framework and pore-filling material [3c].

The N$_2$ adsorption–desorption isotherms of MCM-41 and Mo-MCM-41 (not shown) were of type IV according to the IUPAC classification [24], characteristic of mesoporous solids (pore width between 2 and 50 nm). MCM-41 gave a BET specific surface area of 811 m^2 g^{-1}, a total pore volume of 0.69 cm^3 g^{-1}, and a mode pore width of 4.3 nm. The isotherm of the grafted material revealed only slightly lower N$_2$ uptake, leading to a specific surface area of 797 m^2 g^{-1}, a total pore volume of 0.67 cm^3 g^{-1}, and the same mode pore width as MCM-41. The similarity in the texture properties of the two materials can be attributed to the relatively small size of the grafted complexes in Mo-MCM-41 combined with the low loading.
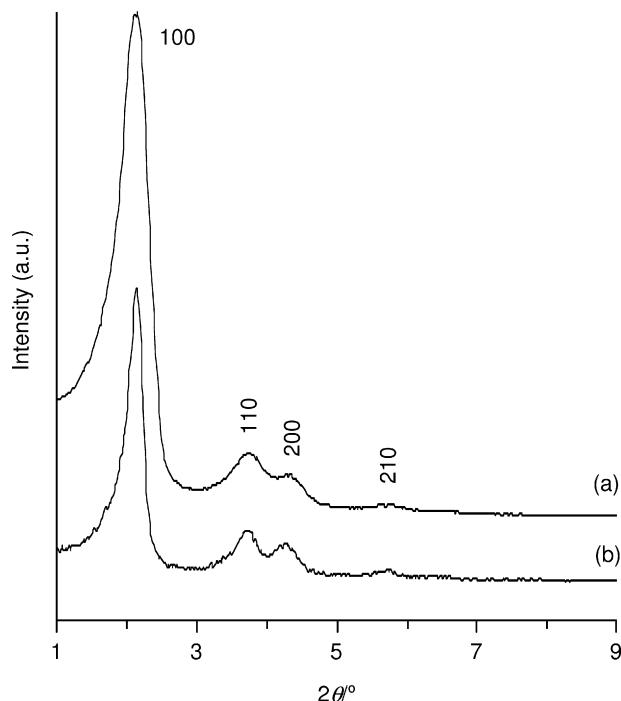

Fig. 1. Powder XRD patterns of (a) calcined (pristine) MCM-41 and (b) Mo-MCM-41.

Preliminary evidence for the presence of surface-grafted species in Mo-MCM-41 was obtained from the ^{29}Si MAS NMR spectra (Fig. 2). Unmodified MCM-41 displays two broad overlapping resonances in the ^{29}Si MAS NMR spectrum at −100.7 and −109.7 ppm corresponding to Q^3 and Q^4 species of the silica framework [Q^n = Si(OSi)$_n$(OH)$_{4-n}$]. A weak shoulder is observed at −91.4 ppm for the Q^2 species. Application of cross-polarisation results in a marked increase in the relative intensities of the Q^2 and Q^3 peaks
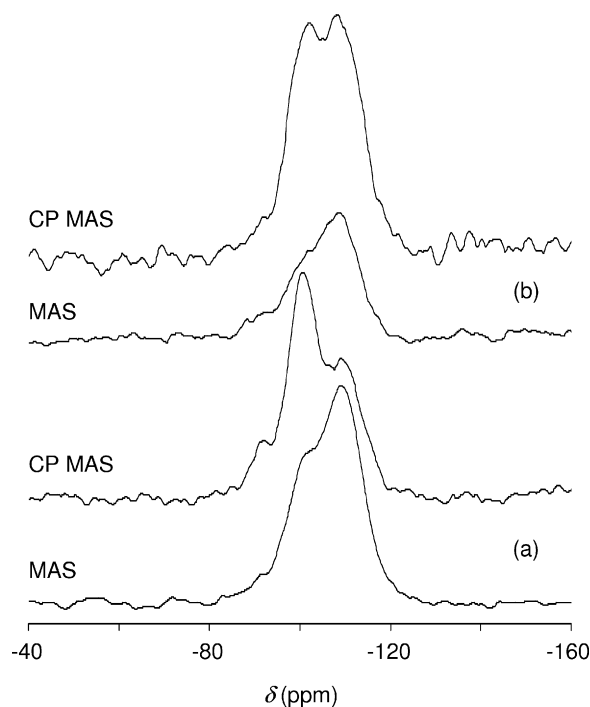

Fig. 2. ^{29}Si MAS and CP MAS NMR spectra of (a) calcined (pristine) MCM-41 and (b) Mo-MCM-41.

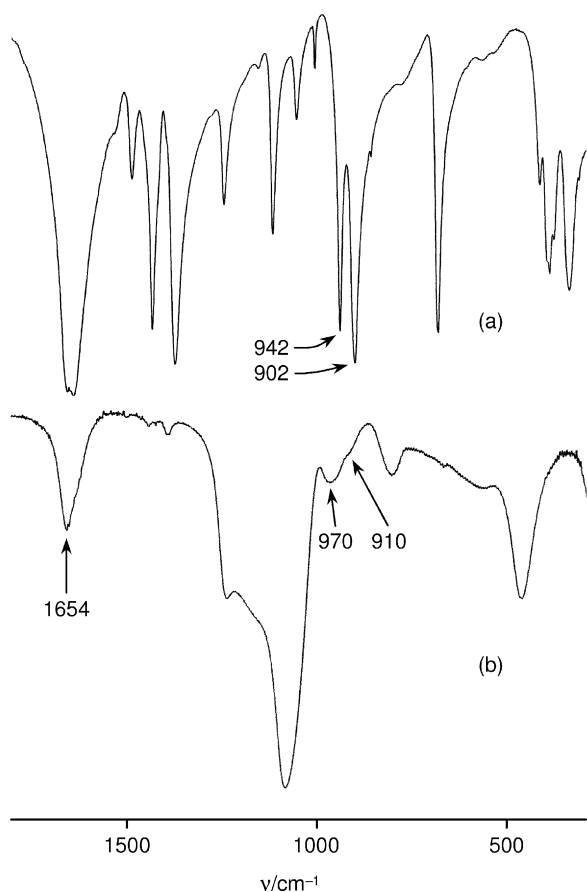**Fig. 3.** Infrared spectra (transmission mode) of (a) $MoO_2Cl_2(dmf)_2$ (**1**) and (b) Mo-MCM-41.

relative to that for the Q^4 peak, which is consistent with the Q^2 and Q^3 sites being associated with geminal silandiols and single Si–OH groups, respectively. Treatment of MCM-41 with **1** in dichloromethane results in a reduction of the Q^2 and Q^3 resonances relative to the Q^4 resonance, especially noticeable in the ^{29}Si CP MAS NMR spectrum. This suggests that a significant number of surface siloxy groups in the original material were chemically modified by nucleophilic substitution of labile chloro ligands in complex **1**, resulting in Mo–O–Si linkages.

The ^{13}C CP MAS NMR spectrum of complex **1** showed relatively sharp signals for the dmf carbonyl and methyl groups (not shown). The original signal of dmf carbonyl at 162.4 ppm (CDCl$_3$) was shifted downfield to 167.3 ppm in the solid state NMR spectrum of **1**, implying the electrophilic activation of the dmf carbonyl by coordination to the Lewis acidic metal centre. The three dmf signals in the spectrum of Mo-MCM-41 were broader and shifted upfield by 2–3 ppm compared with the signals for **1**. Although the signal of dmf carbonyl is still shifted downfield slightly compared with that for dmf in CDCl$_3$, the difference is too small to infer whether the molecules are coordinated to the metal centre or not. The IR spectrum of Mo-MCM-41 was more informative in this respect (Fig. 3), since an absorption band with medium intensity was observed at 1654 cm^{-1} for the carbonyl stretching vibration, in agreement with that exhibited by complex **1** (1653 cm^{-1}). The lowering of the carbonyl frequency from ca. 1670 cm^{-1} for dmf to 1654 cm^{-1} is an indication for coordination through the oxygen atom. For frequencies in the range 300–1300 cm^{-1}, the IR spectrum of Mo-MCM-41 is dominated by the characteristic bands of the MCM-41 support [3c], and only a weak shoulder at 910 cm^{-1} may be attributed to the

grafted species. Complexes of the type $MoO_2X_2L_n$, with a distorted octahedral geometry and a *cis*-dioxo unit, usually exhibit a pair of strong IR bands in the range 900–950 cm^{-1}, assigned to asymmetric and symmetric Mo=O stretching vibrations. Complex **1**, for example, exhibits v_{asym}(Mo=O) at 902 cm^{-1} and v_{sym}(Mo=O) at 942 cm^{-1} (Fig. 3). The band at 910 cm^{-1} for Mo-MCM-41 may therefore be assigned to v_{asym}(Mo=O) of a surface *cis*-dioxomolybdenum complex. The expected v_{sym}(Mo=O) band around 940 cm^{-1} is not observed due to overlap with a broad band with medium/weak intensity at 970 cm^{-1}, which may be assigned to Si–O vibrations in silanols and/or ≡Si–O–Mo moieties.

Mo K-edge EXAFS studies were carried out to get a more conclusive picture of the average structural environment of the molybdenum centres in Mo-MCM-41. Analysis of the raw k^3-weighted EXAFS data for complex **1** gave a first coordination sphere of 1.8 oxygen atoms at 1.70 Å, 2.0 oxygen atoms at 2.32 Å and 2.0 chlorine atoms at 2.37 Å (Fig. 4, Table 1), which is consistent with the expected distorted octahedral coordination geometry consisting of a *cis*-MoO$_2$ unit, two chlorine atoms and two dmf oxygen atoms. The refined Mo=O and Mo–Cl distances are in reasonable agreement with the crystallographic values of 1.68 and 2.34 Å [26], while the Mo–O$_{dmf}$ distance is significantly longer than the reported value of 2.20 Å. The EXAFS-derived distance may be unreliable due to high correlations between the parameters for this shell and those for the chlorine shell. A substantially different model was required for a good fit to the Mo K-edge EXAFS of Mo-MCM-41, comprising oxygen shells at 1.71, 1.97 and 2.25 Å (Fig. 4, Table 1). These distances are very similar to those found previously for MoO$_2$Cl$_2$(thf)$_2$ grafted onto MCM-41 at a molybdenum loading of 1 wt.% [3c]. On comparing the Fourier transforms of the k^3-weighted EXAFS data for complex **1** and Mo-MCM-41 it is obvious that the Mo–Cl bonds were disrupted during the grafting process. Indeed, no acceptable fit could be obtained for a chlorine shell around 2.35 Å. The distance for the first oxygen shell is consistent with Mo=O bonds and the refined coordination number suggests that most of the Mo atoms are present as dioxo species. The second shell may be attributed to the bridging oxygen atoms in Mo–O–Si linkages and the third shell to oxygen atoms of coordinated dmf molecules. These data suggest that most of the Mo atoms are present as bipodally anchored dioxomolybdenum(VI) species, which may have the distorted octahedral geometry schematically represented in Fig. 5. According to this model we might expect the Mo···Si interaction to make a significant contribution to the EXAFS. However, attempts to fit a fourth shell for Si atoms between 3 and 3.5 Å were unsuccessful, which may be due to disorder in the Mo–O–Si bonds. On the other hand, a statistically significant improvement in the fit was obtained after inclusion of a shell for Mo atoms at 3.33 Å, with a refined coordination number of 0.25 (Table 1). This suggests that a small fraction (ca. 15% or less) of the surface species may be oxo-bridged dimers similar to those reported for MoO$_2$Cl$_2$(thf)$_2$ grafted onto MCM-41 (at a loading of 4 wt.% Mo) [3c] and MoO$_2$(acac)$_2$ immobilised in polymer supports carrying hydroxypropylaminomethyl pyridine ligands [27]. As proposed for the polymer supported complexes [27], the oxo-bridged dimers in Mo-MCM-41 may be mixed valence (Mo^V/Mo^{VI}), which may explain the pale blue color of the isolated material.

3.2. Catalytic tests

The dioxomolybdenum(VI) complex **1** and the derivatised material Mo-MCM-41 catalyse the epoxidation of unfunctionalised olefins, namely cyclooctene, 1-octene, *trans*-2-octene, (*R*)-(+)-limonene, norbornene, α-pinene and styrene, using *t*BuOOH or CuOOH as oxygen donor, from ambient to 55 °C, and approximately atmospheric pressure. Complex **1** exhibits excellent selectivity to the epoxidation of cyclooctene (Cy8), used as a model substrate,
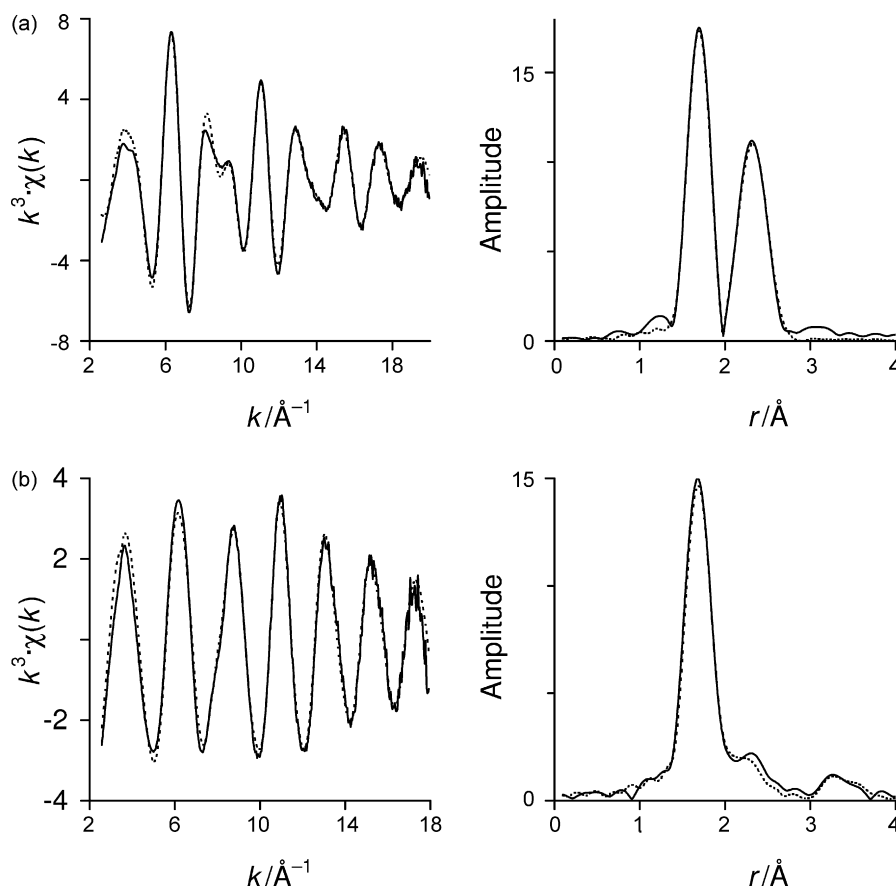
Fig. 4. Mo K-edge k^3-weighted EXAFS and Fourier transforms of (a) MoO$_2$Cl$_2$(dmf)$_2$ (**1**) (sum of two scans) and (b) Mo-MCM-41 (sum of four scans). The solid lines represent the experimental data and the dashed lines show the fits obtained using the parameters given in Table 1.

giving cyclooctene oxide as the only reaction product in all experiments. Under the same reaction conditions but without a catalyst, no significant olefin conversion is observed. Using equimolar amounts of oxidant and Cy8, the turnover frequencies (TOF) were 291 mol mol$_{Mo}^{-1}$ h^{-1} with *t*BuOOH and 211 mol mol$_{Mo}^{-1}$ h^{-1} with CuOOH, at 25 °C and in the absence of additional co-solvent (Table 2). No reaction took place when 30% aq. H$_2$O$_2$ was used as the oxygen donor instead of an alkyl hydroperoxide. Increasing the molar ratio of Cy8:*t*BuOOH from 1:1 to 1:1.6 led to an increase in TOF from 291 to 689 mol mol$_{Mo}^{-1}$ h^{-1}. When, additionally, the reaction temperature was raised to 55 °C, a TOF of 1003 mol mol$_{Mo}^{-1}$ h^{-1} was reached. Under these conditions the epoxide

yield after 5 min reaction was 84%, which became quantitative shortly afterwards.

The catalytic activity of complex **1** is quite outstanding compared with that typically exhibited by mononuclear MoO$_2$X$_2$L$_n$ complexes (X = F, Cl, Br, alkyl; L = neutral monodentate or bidentate N,O-ligand) used as catalysts in the same reaction, under similar conditions. Generally, TOFs of less than 600 mol mol$_{Mo}^{-1}$ h^{-1} are found for these types of complexes bearing Lewis-base ligands (L) [28]. The solvent adduct MoO$_2$Br$_2$(CH$_3$CN)$_2$ gives a TOF of about 200 mol mol$_{Mo}^{-1}$ h^{-1} when a reaction temperature of 55 °C is used [14d]. The kinetic profiles of cyclooctene conversion in the presence of complex **1** (at 25 or 55 °C) show a major consumption of olefin during the first few minutes of the reaction followed by a significant decrease in the reaction rate (Fig. 6). Similar kinetic features have been reported for cyclooctene epoxidation with *t*BuOOH catalysed by several MoO$_2$X$_2$L$_n$ complexes [29]. The strong tail off in reaction rate has been attributed to catalyst deactivation due to the pronounced water sensitivity of selected complexes (such as the bis(acetonitrile)dibromo complex mentioned above [14d]) and/or relatively strong inhibition by *tert*-butanol (*t*BuOH), which is formed in the reaction of *t*BuOOH [29].

The influence of additional aprotic solvents on the catalytic performance of complex **1** was investigated using *n*-hexane, a non-polar, non-coordinating solvent, dichloromethane (dcm), a polar, non-coordinating solvent, and dmf, a polar, coordinating solvent, at 25 °C. Cyclooctene epoxide was the only observed reaction product in all three systems. Catalytic activity improved significantly when dcm was used as the co-solvent (Fig. 6), leading to a TOF of 806 mol mol$_{Mo}^{-1}$ h^{-1} (Table 2). The higher reaction rate may

Table 1
Mo K-edge EXAFS-derived structural parameters.

Compound	Atom	CN[a]	r (Å)	$2\sigma^2$ [b] (Å^2)	E_f[c] (eV)	R[d] (%)
MoO$_2$Cl$_2$(dmf)$_2$ (**1**)	O	1.8(1)	1.705(1)	0.0033(1)	4.8(4)	13.3
	O	2.0(2)	2.322(9)	0.0085(3)		
	Cl	2.0(2)	2.375(3)	0.0250(49)		
Mo-MCM-41	O	1.7(1)	1.710(1)	0.0030(2)	3.6(4)	15.1
	O	1.7(2)	1.973(5)	0.0166(12)		
	O	1.6(2)	2.246(7)	0.0166(17)		
	Mo	0.25(14)	3.331(11)	0.0096(19)		

[a] CN = coordination number. Values in parentheses are statistical errors generated in EXCURVE. The true errors in coordination numbers are likely to be of the order of 20%; those for the interatomic distances ca. 1.5% [25].

[b] Debye–Waller factor; σ = root-mean-square internuclear separation.

[c] E_f = edge position (Fermi energy), relative to calculated vacuum zero.

[d] $R = (\int [\Sigma^{theory} - \Sigma^{exptl}] k^3 \, dk / [\Sigma^{exptl}] k^3 \, dk) \times 100\%$.

Table 2
Catalytic performance of complex **1** and Mo-MCM-41 in the epoxidation of cyclooctene (Cy8) at 25 °C.

Catalyst	Oxidant	Ratio Cy8/oxidant	Solvent	TOF[a] (mol mol$_{Mo}^{-1}$ h^{-1})	Conv.[b] (%)
1	tBuOOH	1:1	None	291	62
		1:1.6	None	689	81
		1:1.6[c]	None	1003	100 (100[d])
		1:1	dmf	5	6
		1:1	dcm [e]	806	97
		1:1	n-Hexane	33	44
	CuOOH	1:1	None	211	49
Mo-MCM-41	tBuOOH	1:1	None	306	57
		1:1.6[c]	None	241	100 (100[d])
		1:1	dcm	544	91

[a] Turnover frequency calculated at 10 min reaction.
[b] Cyclooctene conversion after 24 h reaction.
[c] Reaction carried out at 55 °C.
[d] Conversion for second 24 h reaction run.
[e] Dichloromethane.

be partly explained by the fact that complex **1** is evidently more soluble in the system containing dcm. When n-hexane was used, the reaction was much slower (TOF = 33 mol mol$_{Mo}^{-1}$ h^{-1}), and the conversion reached at 6 h was 43%, compared with 96% for dcm. The lower solubility of complex **1** in n-hexane may account for the difference in the reaction rates for the two systems. An even lower catalytic activity was found with dmf as co-solvent, leading to 6% conversion at 24 h. These results may be due to unfavourable interactions between the olefin/oxidant molecules and the dmf-solvated and coordinated molybdenum species.

The catalytic stability of **1** was investigated by carrying out two 24 h runs at 55 °C, using a substrate:oxidant molar ratio of 1:1.6. After the first run, the reaction vessel was recharged with substrate and oxidant in identical amounts to those used in the first run. Initially, the reaction was somewhat slower in the second run, but after 1 h the kinetic curves converged to give the same conversion of about 98% at 6 h (Fig. 6). Since the catalyst was not separated from the reaction products, the accumulation of tBuOH, a possible competitive inhibitor, could retard the reaction and cause a lower

initial reaction rate. The reaction of complex **1** with different oxygen sources was studied by Mimoun and co-workers [15]. In the presence of H$_2$O$_2$ or Ph$_3$COOH, monoperoxo and bisperoxo complexes of the type MoO(O$_2$)Cl$_2$L$_2$ and MoO(O$_2$)$_2$L$_2$ are formed (L = dmf, H$_2$O), which exhibit poor selectivities as catalysts for olefin epoxidation. The epoxide selectivities are much higher when tBuOOH is used as the oxygen source, which led Mimoun and co-workers to conclude that alkyl-peroxidic rather than peroxo species are intermediates in the reaction. Accordingly, recent experimental and theoretical studies by Kühn and co-workers have shown that MoO$_2$X$_2$L$_n$ (X = Cl, Br, CH$_3$) complexes carrying Lewis-base ligands undergo an equilibrium reaction with excess tBuOOH to give seven-coordinate Mo^{VI} η^1-alkylperoxo complexes that selectively catalyse the epoxidation of olefins [30]. So far, attempts to isolate the species formed from the reaction of MoO$_2$X$_2$L$_n$ (L = dmf or Lewis-base) with excess tBuOOH have been unsuccessful, with the starting compound always being recovered unchanged [15,30]. In the present work, complex **1** was treated with a 150-fold excess of tBuOOH (5.5 M in n-decane) in 1,2-dichloroethane. When working up the reaction mixture, a solid was obtained which was tested as a catalyst
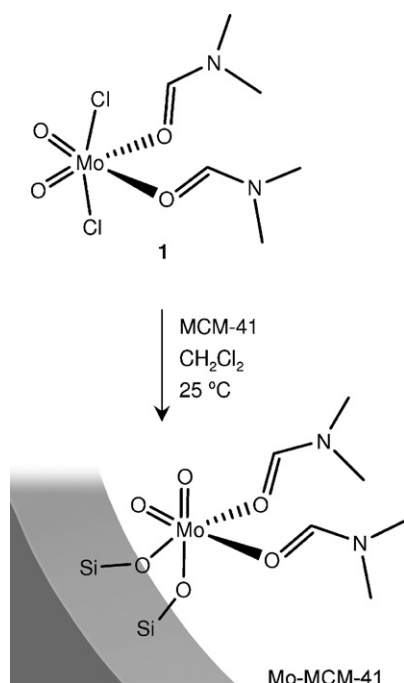

Fig. 5. Representation of the predominant surface species present in Mo-MCM-41 as evidenced by FTIR spectroscopy, ^{13}C and ^{29}Si MAS NMR, and Mo K-edge EXAFS.
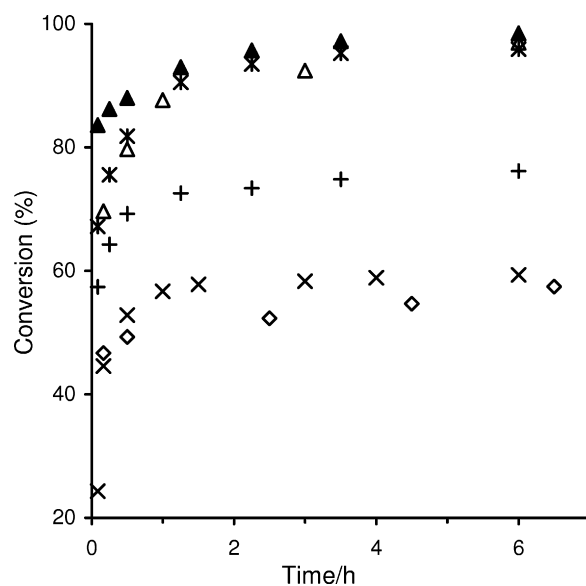

Fig. 6. Kinetic profiles of cyclooctene epoxidation with tBuOOH: 25 °C, no co-solvent, **1**:substrate:oxidant = 0.01:1:1 (×), **1**:substrate:oxidant = 0.01:1:1.6 (+), and **1***:substrate:oxidant = 0.01:1:1 (◇); 25 °C, dichloromethane, **1**:substrate:oxidant = 0.01:1:1 (∗); 55 °C, no co-solvent, **1**:substrate:oxidant = 0.01:1:1.6, run 1 (▲) and run 2 (△).
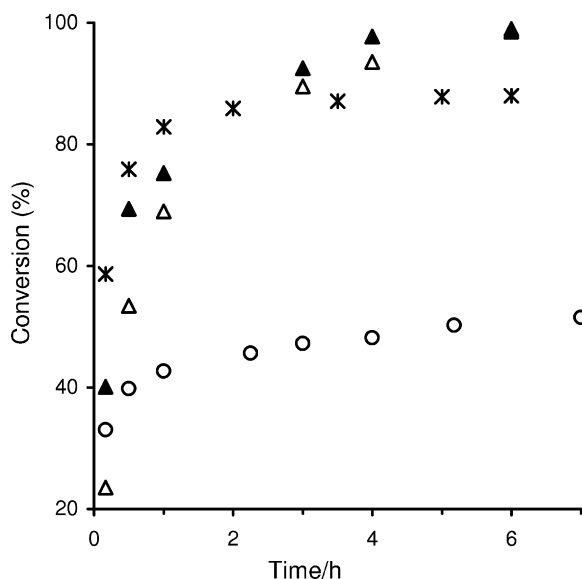
Fig. 7. Kinetic profiles of cyclooctene epoxidation with *t*BuOOH in the presence of Mo-MCM-41: 25 °C, substrate:oxidant = 1:1, no co-solvent (○) or in the presence of dichloromethane (*); at 55 °C, substrate:oxidant = 1:1.6, no co-solvent, run 1 (▲) and run 2 (△).

for cyclooctene oxidation at 25 °C using a catalyst:Cy8:*t*BuOOH molar ratio of 0.01:1:1. As expected from the literature work cited above, the kinetic profile (referred to as **1*** in Fig. 6) was quite similar to that obtained for the as-synthesised complex **1**, reaching practically the same conversion of 57–59% after 6 h and giving the epoxide as the only reaction product.

When used as a catalyst in the reaction of Cy8 with *t*BuOOH (in equimolar amounts) at 25 °C, the derivatised material Mo-MCM-41 gave a TOF (306 mol mol$_{Mo}^{-1}$ h^{-1}) and kinetic profile very similar to those exhibited by complex **1** (Table 2, Fig. 7). As found for complex **1**, the use of dichloromethane as a co-solvent considerably improved the catalytic performance of Mo-MCM-41: 88% conversion was achieved within 6 h reaction with dcm compared with 50% without additional solvent (Fig. 7). The higher reaction rate observed for dcm, a moderately polar solvent, may be partly due to the enhanced adsorption of the reagents on the catalyst surface: the driving force may be specific interactions between dcm-solvated reagents and the (possibly moderately polar) inorganic–organic surface. On the other hand, the polarisability of molybdenum surface species caused by the presence of the dcm molecules may affect the catalytic activity.

After the catalytic reaction the solid catalyst was separated from the reaction products by centrifugation, washed with *n*-hexane and dried at room temperature. ICP-AES of the recovered solid indicated a 6% decrease in the Mo content relative to the fresh catalyst. A leaching test was performed for the reaction of Cy8 without co-solvent by filtering the reaction mixture (using a Whatman 0.2 μm PVDF w/GMF membrane) at the reaction temperature (25 °C), and leaving the solution to react further. A 3% increase in conversion was observed between 10 min and 7 h, compared with 19% in the presence of Mo-MCM-41. These results suggest that epoxidation in the presence of Mo-MCM-41 (for the first run) is, to a relatively small extent, homogeneously catalysed by leached molybdenum species. During the first catalytic run the nucleophilic reagent *t*BuOOH may react with the small number of oxo-bridged bimetallic structures, resulting in cleavage of the Mo–O–Mo bridge and leaching of some Mo [27].

To further assess the recyclability of Mo-MCM-41, the solid was recovered from a reaction run at 55 °C, with a Cy8:*t*BuOOH molar

ratio of 1:1.6, and used in a separately prepared batch. This procedure avoids the accumulation of *t*BuOH in consecutive runs. The catalytic performance in the two runs was similar to that observed for complex **1**. Initially, the reaction was slightly slower in the second run, but after 1 h the kinetic curves converged to give the same conversion of about 99% at 6 h (Fig. 7). The stability and recyclability of Mo-MCM-41 in catalytic olefin epoxidation seems to be much superior to that found previously for MoO$_2$Cl$_2$(thf)$_2$ grafted onto MCM-41 at a molybdenum loading of 1 wt.% [3c], and is on a par with that found for oxodiperoxo molybdenum chelate complexes covalently anchored onto MCM-41 [31].

Cyclooctene is arguably the easiest common olefin to epoxidise [2c], and therefore it is important to consider other olefins as substrates when assessing the performance of potentially interesting oxidation catalysts. Complex **1** and Mo-MCM-41 were tested as catalysts for the oxidation of a series of linear and cyclic olefins at 55 °C without a co-solvent, using a catalyst:substrate:*t*BuOOH molar ratio of 1:100:158 (Table 3). A comparison of the catalytic activities for the epoxidation of the linear octenes indicates that both catalysts are more active in the epoxidation of internal double bonds than of terminal ones, as would be expected based on mechanistic findings [29,30]. The activity of the catalyst for the conversion of 1-octene appears to be roughly similar to that recently reported for a mesostructured Mo-SBA-15 catalyst with an Mo content of 2.3 wt.% [32]. No correlation could be established between the polarity of the substrate molecules and the catalytic activity (this could be important since in the absence of solvent the volume of substrate in the reaction medium is considerable): for example, the dielectric constants of limonene and pinene are similar (2–3, at 20 °C), while the former is more reactive than the latter. α-Pinene and styrene are the least reactive possibly because of steric/electronic effects: the electron density of the olefinic bond of styrene may be affected by the aromatic substituent group, while in the case of α-pinene the proximal dimethyl bridge may cause steric hindrance. The reactions of norbornene, Cy8, 1-octene and *trans*-2-octene gave the corresponding epoxide as the only product throughout 24 h reaction. In contrast, the reactions of α-pinene and styrene were not selective to the corresponding epoxide, under the applied reaction conditions, originating a wide spectrum of products, which included campholenic aldehyde from α-pinene, and benzaldehyde and phenyl acetaldehyde from styrene. The reaction of (R)-(+)-limonene gave limonene oxide to a greater extent

Table 3
Catalytic performance of complex **1** and Mo-MCM-41 in the oxidation of olefins, at 55 °C, using a catalyst:substrate:oxidant molar ratio of 1:100:158.

Catalyst	Olefin	Conversion (%) 6/24 h	Selectivity[a] (%) 6/24 h
1	Cyclooctene	98/100	100/100
	1-Octene	29/48	100/100
	trans-2-Octene	82/96	100/100
	(R)-(+)-Limonene	98/99	30/39[b]
	Norbornene	98/100	100/100
	α-Pinene	28/45	59/76[c]
	Styrene	25/50	20/18[d]
Mo-MCM-41	Cyclooctene	100/100	100/100
	1-Octene	36/58	100/100
	trans-2-Octene	83/94	100/100
	(R)-(+)-Limonene	78/95	100/53[b]
	Norbornene	97/100	100/100
	α-Pinene	15/35	37/51[c]
	Styrene	19/45	32/25[d]

[a] Selectivity to epoxide, unless indicated otherwise.
[b] By-products include 8,9-*p*-menthen-1,2-diol.
[c] Selectivity to campholenic aldehyde (no epoxide was detected and several other products were formed, which were not identified).
[d] Selectivity to benzaldehyde (no epoxide was detected and several other products were formed, such as phenyl acetaldehyde).

in the presence of Mo-MCM-41, and after 24 h 8,9-*p*-menthen-1,2-diol was formed as a by-product in 32% yield with complex **1** and 45% yield with Mo-MCM-41. When equimolar amounts of limonene and *t*BuOOH were used, with dcm as the co-solvent and a reaction temperature of 25 °C, the reaction was 100% selective to limonene oxide at 59% and 45% conversion (24 h) in the presence of **1** and Mo-MCM-41, respectively.

4. Conclusions

This work has shown that the complex $MoO_2Cl_2(dmf)_2$ is an effective precursor for the deposition of oxomolybdenum species onto mesoporous silica by the so-called molecular designed dispersion method [12]. The low surface concentration of $0.17 \, Mo/nm^2$ ensures that most of the surface structures are isolated, monometallic dioxomolybdenum(VI) species. Despite the low surface coverage, the catalytic activity of the material for the selective epoxidation of cyclooctene with *t*BuOOH under mild conditions compares favourably with other silica-supported Mo^{VI} complexes reported in the literature. Moreover, the performance is similar to that exhibited by $MoO_2Cl_2(dmf)_2$ in homogeneous phase, which suggests that most, if not all, of the Mo centres in the supported catalyst are active and accessible. Demanding olefins such as limonene can also be epoxidised with high selectivity, albeit with only fair conversion. Another important factor is the stability and recyclability of the catalyst under the reaction conditions used. Leaching tests indicate that the catalytic reaction is mainly heterogeneous in nature, with only a small contribution (in the first catalytic run) from active species leached into the liquid phase. These results are consistent with most of the Mo atoms being anchored to the surface through covalent Si–O–Mo linkages.

Acknowledgements

References

[1] (a) N.D. Spencer, C.J. Pereira, R.K. Grasselli, J. Catal. 126 (1990) 546;
(b) M.A. Banares, J.L.G. Fierro, J.B. Moffat, J. Catal. 142 (1993) 406;
(c) A. Parmaliana, V. Sokolovskii, D. Miceli, F. Arena, N. Giordano, J. Catal. 148 (1994) 514.

[2] (a) A.N. Desikan, W. Zhang, S.T. Oyama, J. Catal. 157 (1995) 740;
(b) N.C. Ramani, D.L. Sullivan, J.G. Ekerdt, J.-M. Jehng, I.E. Wachs, J. Catal. 176 (1998) 143;
(c) P.C. Bakala, E. Briot, L. Salles, J.-M. Brégeault, Appl. Catal. A: Gen. 300 (2006) 91.

[3] (a) M.A. Banares, H.C. Hu, I.E. Wachs, J. Catal. 150 (1994) 407;
(b) M. Seman, J.N. Kondo, K. Domen, R. Radhakrishnan, S.T. Oyama, J. Phys. Chem. B 106 (2002) 12965;
(c) C.D. Nunes, A.A. Valente, M. Pillinger, J. Rocha, I.S. Gonçalves, Chem. Eur. J. 9 (2003) 4380.

[4] F. Arena, A. Parmaliana, J. Phys. Chem. 100 (1996) 19994.

[5] (a) R. Radhakrishnan, C. Reed, S.T. Oyama, M. Seman, J.N. Kondo, K. Domen, Y. Ohminami, K. Asakura, J. Phys. Chem. B 105 (2001) 8519;

(b) J. Jarupatrakorn, M.P. Coles, T.D. Tilley, Chem. Mater. 17 (2005) 1818;
(c) N. Ohler, A.T. Bell, J. Phys. Chem. B 110 (2006) 2700;
(d) S. Chempath, Y. Zhang, A.T. Bell, J. Phys. Chem. C 111 (2007) 1291;
(e) E.L. Lee, I.E. Wachs, J. Phys. Chem. C 112 (2008) 6487.

[6] (a) Y. Iwasawa, Adv. Catal. 35 (1987) 187;
(b) Y. Kikutani, J. Mol. Catal. A: Chem. 142 (1999) 247;
(c) S. Braun, L.G. Appel, V.L. Camorim, M. Schmal, J. Phys. Chem. B 104 (2000) 6584;
(d) S. Higashimoto, Y. Hu, R. Tsumura, K. Iino, M. Matsuoka, H. Yamashita, Y.G. Shul, M. Che, M. Anpo, J. Catal. 235 (2005) 272.

[7] (a) M. del Arco, S.R.G. Carrazán, C. Martín, I. Martín, V. Rives, P. Malet, J. Mater. Chem. 3 (1993) 1313;
(b) G. Mestl, T.K.K. Srinivasan, Catal. Rev. Sci. Eng. 40 (1998) 451;
(c) P.C. Bakala, E. Briot, J.-Y. Piquemal, J.-M. Brégeault, P. Beaunier, Catal. Commun. 8 (2007) 1447.

[8] (a) J.M. Thomas, R. Raja, D.W. Lewis, Angew. Chem. Int. Ed. 44 (2005) 6456;
(b) K.R. Jain, F.E. Kühn, Dalton Trans. (2008) 2221.

[9] (a) C.C. Williams, J.G. Ekerdt, J.-M. Jehng, F.D. Hardcastle, A.M. Turek, I.E. Wachs, J. Phys. Chem. 95 (1991) 8781;
(b) C. Louis, M. Che, M. Anpo, J. Catal. 141 (1993) 453.

[10] B. Griffe, A. Sierraalta, F. Ruette, J.L. Brito, J. Mol. Struct. (Theochem.) 625 (2003) 59.

[11] Q. Zhuang, A. Fukuoka, T. Fujimoto, K. Tanaka, M. Ichikawa, J. Chem. Soc. Chem. Commun. (1991) 745.

[12] O. Collart, P. Van Der Voort, E.F. Vansant, E. Gustin, A. Bouwen, D. Schoemaker, R.R. Rao, B.M. Weckhuysen, R.A. Schoonheydt, Phys. Chem. Chem. Phys. 1 (1991) 4099.

[13] I.J. Shannon, T. Maschmeyer, R.D. Oldroyd, G. Sankar, J.M. Thomas, H. Perrot, J.-P. Balkdjian, M. Che, J. Chem. Soc. Faraday Trans. 94 (1998) 1495.

[14] (a) M.L. Larson, F.W. Moore, Inorg. Chem. 5 (1966) 801;
(b) R.J. Butcher, H.P. Gunz, R.G.A.R. Maclagan, H.K.J. Powell, C.J. Wilkins, Y.S. Hian, J. Chem. Soc. Dalton Trans. (1975) 1223;
(c) F.J. Arnáiz, R. Aguado, J. Sanz-Aparicio, M. Martinez-Ripoll, Polyhedron 13 (1994) 2745;
(d) F.E. Kühn, E. Herdtweck, J.J. Haider, W.A. Herrmann, I.S. Gonçalves, A.D. Lopes, C.C. Romão, J. Organomet. Chem. 583 (1999) 3.

[15] P. Chaumette, H. Mimoun, L. Saussine, J. Fischer, A. Mitschler, J. Organomet. Chem. 250 (1983) 291.

[16] K. Jeyakumar, D.K. Chand, Appl. Organomet. Chem. 20 (2006) 840.

[17] R. Sanz, J. Escribano, M.R. Pedrosa, R. Aguado, F.J. Arnáiz, Adv. Synth. Catal. 349 (2007) 713.

[18] J.P. Lourenço, A. Fernandes, C. Henriques, M.F. Ribeiro, Micropor. Mesopor. Mater. 94 (2006) 56.

[19] (a) M. Kruk, M. Jaroniec, Langmuir 13 (1997) 6267;
(b) M. Kruk, V. Antochshuk, M. Jaroniec, J. Phys. Chem. B 103 (1999) 10670.

[20] A. Tenderholt, B. Hedman, K.O. Hodgson, Proceedings of the 13th International Conference on X-ray Absorption Fine Structure (XAFS13) 882, 2007, pp. 105–107.

[21] N. Binsted, EXCURV98, CCLRC Daresbury Laboratory computer programme, 1998.

[22] (a) S.J. Gurman, N. Binsted, I. Ross, J. Phys. C 17 (1984) 143;
(b) S.J. Gurman, N. Binsted, I. Ross, J. Phys. C 19 (1986) 1845.

[23] K.P. O'Donnell, J.F.W. Mosselmans, R.W. Martin, S. Pereira, M.E. White, J. Phys.: Condens. Matter 13 (2001) 6977.

[24] S.J. Gregg, K.S.W. Sing, Adsorption, Surface Area and Porosity, 2nd ed., Academic Press, London, 1982.

[25] J. Evans, J.T. Gauntlett, J.F.W. Mosselmans, Faraday Discuss. Chem. Soc. 107 (1990) 107.

[26] L.R. Florian, E.R. Corey, Inorg. Chem. 7 (1968) 722.

[27] M.M. Miller, D.C. Sherrington, J. Catal. 152 (1995) 368.

[28] C.C.L. Pereira, S.S. Balula, F.A. Almeida Paz, A.A. Valente, M. Pillinger, J. Klinowski, I.S. Gonçalves, Inorg. Chem. 46 (2007) 8508, and references cited therein.

[29] (a) A.A. Valente, J. Moreira, A.D. Lopes, M. Pillinger, C.D. Nunes, C.C. Romão, F.E. Kühn, I.S. Gonçalves, New J. Chem. 28 (2004) 308;
(b) A. Al-Ajlouni, A.A. Valente, C.D. Nunes, M. Pillinger, A.M. Santos, J. Zhao, C.C. Romão, I.S. Gonçalves, F.E. Kühn, Eur. J. Inorg. Chem. (2005) 1716.

[30] (a) F.E. Kühn, M. Groarke, É. Bencze, E. Herdtweck, A. Prazeres, A.M. Santos, M.J. Calhorda, C.C. Romão, I.S. Gonçalves, A.D. Lopes, M. Pillinger, Chem. Eur. J. 8 (2002) 2370;
(b) M. Groarke, I.S. Gonçalves, W.A. Herrmann, F.E. Kühn, J. Organomet. Chem. 649 (2002) 108.

[31] (a) M. Jia, W.R. Thiel, Chem. Commun. (2002) 2392;
(b) M. Jia, A. Seifert, W.R. Thiel, Chem. Mater. 15 (2003) 2174.

[32] J.A. Melero, J. Iglesias, J.M. Arsuaga, J. Sainz-Pardo, P. de Frutos, S. Blazquez, Appl. Catal. A: Gen. 331 (2007) 84.